# Measurement of Day and Night Neutrino Energy Spectra at SNO and Constraints on Neutrino Mixing Parameters

Q. R. Ahmad,[17] R. C. Allen,[4] T. C. Andersen,[6] J. D. Anglin,[10] J. C. Barton,[11,*] E. W. Beier,[12] M. Bercovitch,[10] J. Bigu,[7] S. D. Biller,[11] R. A. Black,[11] I. Blevis,[5] R. J. Boardman,[11] J. Boger,[3] E. Bonvin,[14] M. G. Boulay,[9,14] M. G. Bowler,[11] T. J. Bowles,[9] S. J. Brice,[9,11] M. C. Browne,[17,9] T. V. Bullard,[17] G. Bühler,[4] J. Cameron,[11] Y. D. Chan,[8] H. H. Chen,[4,†] M. Chen,[14] X. Chen,[8,11] B. T. Cleveland,[11] E. T. H. Clifford,[14] J. H. M. Cowan,[7] D. F. Cowen,[12] G. A. Cox,[17] X. Dai,[11] F. Dalnoki-Veress,[5] W. F. Davidson,[10] P. J. Doe,[17,9,4] G. Doucas,[11] M. R. Dragowsky,[9,8] C. A. Duba,[17] F. A. Duncan,[14] M. Dunford,[12] J. A. Dunmore,[11] E. D. Earle,[14,1] S. R. Elliott,[17,9] H. C. Evans,[14] G. T. Ewan,[14] J. Farine,[7,5] H. Fergani,[11] A. P. Ferraris,[11] R. J. Ford,[14] J. A. Formaggio,[17] M. M. Fowler,[9] K. Frame,[11] E. D. Frank,[12] W. Frati,[12] N. Gagnon,[11,9,8,17] J. V. Germani,[17] S. Gil,[2] K. Graham,[14] D. R. Grant,[5] R. L. Hahn,[3] A. L. Hallin,[14] E. D. Hallman,[7] A. S. Hamer,[9,14] A. A. Hamian,[17] W. B. Handler,[14] R. U. Haq,[7] C. K. Hargrove,[5] P. J. Harvey,[14] R. Hazama,[17] K. M. Heeger,[17] W. J. Heintzelman,[12] J. Heise,[2,9] R. L. Helmer,[16,2] J. D. Hepburn,[14] H. Heron,[11] J. Hewett,[7] A. Hime,[9] M. Howe,[17] J. G. Hykawy,[7] M. C. P. Isaac,[8] P. Jagam,[6] N. A. Jelley,[11] C. Jillings,[14] G. Jonkmans,[7,1] K. Kazkaz,[17] P. T. Keener,[12] J. R. Klein,[12] A. B. Knox,[11] R. J. Komar,[2] R. Kouzes,[13] T. Kutter,[2] C. C. M. Kyba,[12] J. Law,[6] I. T. Lawson,[6] M. Lay,[11] H. W. Lee,[14] K. T. Lesko,[8] J. R. Leslie,[14] I. Levine,[5] W. Locke,[11] S. Luoma,[7] J. Lyon,[11] S. Majerus,[11] H. B. Mak,[14] J. Maneira,[14] J. Manor,[17] A. D. Marino,[8] N. McCauley,[12,11] A. B. McDonald,[14,13] D. S. McDonald,[12] K. McFarlane,[5] G. McGregor,[11] R. Meijer Drees,[17] C. Mifflin,[5] G. G. Miller,[9] G. Milton,[1] B. A. Moffat,[14] M. Moorhead,[11] C. W. Nally,[2] M. S. Neubauer,[12] F. M. Newcomer,[12] H. S. Ng,[2] A. J. Noble,[16,5] E. B. Norman,[8] V. M. Novikov,[5] M. O'Neill,[5] C. E. Okada,[8] R. W. Ollerhead,[6] M. Omori,[11] J. L. Orrell,[17] S. M. Oser,[12] A. W. P. Poon,[8,17,2,9] T. J. Radcliffe,[14] A. Roberge,[7] B. C. Robertson,[14] R. G. H. Robertson,[17,9] S. S. E. Rosendahl,[8] J. K. Rowley,[3] V. L. Rusu,[12] E. Saettler,[7] K. K. Schaffer,[17] M. H. Schwendener,[7] A. Schülke,[8] H. Seifert,[7,17,9] M. Shatkay,[5] J. J. Simpson,[6] C. J. Sims,[11] D. Sinclair,[5,16] P. Skensved,[14] A. R. Smith,[8] M. W. E. Smith,[17] T. Spreitzer,[12] N. Starinsky,[5] T. D. Steiger,[17] R. G. Stokstad,[8] L. C. Stonehill,[17] R. S. Storey,[10] B. Sur,[1,14] R. Tafirout,[7] N. Tagg,[6,11] N. W. Tanner,[11] R. K. Taplin,[11] M. Thorman,[11] P. M. Thornewell,[11] P. T. Trent,[11] Y. I. Tserkovnyak,[2] R. Van Berg,[12] R. G. Van de Water,[9,12] C. J. Virtue,[7] C. E. Waltham,[2] J.-X. Wang,[6] D. L. Wark,[15,11,9] N. West,[11] J. B. Wilhelmy,[9] J. F. Wilkerson,[17,9] J. R. Wilson,[11] P. Wittich,[12] J. M. Wouters,[9] and M. Yeh[3]

(SNO Collaboration)

[1]*Atomic Energy of Canada, Limited, Chalk River Laboratories, Chalk River, Ontario K0J 1J0, Canada*
[2]*Department of Physics and Astronomy, University of British Columbia, Vancouver, British Columbia V6T 1Z1, Canada*
[3]*Chemistry Department, Brookhaven National Laboratory, Upton, New York 11973-5000*
[4]*Department of Physics, University of California, Irvine, California 92717*
[5]*Carleton University, Ottawa, Ontario K1S 5B6, Canada*
[6]*Physics Department, University of Guelph, Guelph, Ontario N1G 2W1, Canada*
[7]*Department of Physics and Astronomy, Laurentian University, Sudbury, Ontario P3E 2C6, Canada*
[8]*Institute for Nuclear and Particle Astrophysics and Nuclear Science Division, Lawrence Berkeley National Laboratory, Berkeley, California 94720*
[9] *Los Alamos National Laboratory, Los Alamos, New Mexico 87545*
[10]*National Research Council of Canada, Ottawa, Ontario K1A 0R6, Canada*
[11]*Department of Physics, University of Oxford, Denys Wilkinson Building, Keble Road, Oxford OX1 3RH, United Kingdom*
[12]*Department of Physics and Astronomy, University of Pennsylvania, Philadelphia, Pennsylvania 19104-6396*
[13]*Department of Physics, Princeton University, Princeton, New Jersey 08544*
[14]*Department of Physics, Queen's University, Kingston, Ontario K7L 3N6, Canada*
[15]*Rutherford Appleton Laboratory, Chilton, Didcot, Oxon OX11 0QX, United Kingdom and University of Sussex, Physics and Astronomy Department, Brighton BN1 9QH, United Kingdom*
[16]*TRIUMF, 4004 Wesbrook Mall, Vancouver, British Columbia V6T 2A3, Canada*
[17]*Center for Experimental Nuclear Physics and Astrophysics, and Department of Physics, University of Washington, Seattle, Washington 98195*

(Received 19 April 2002; published 13 June 2002)

The Sudbury Neutrino Observatory (SNO) has measured day and night solar neutrino energy spectra and rates. For charged current events, assuming an undistorted $^8$B spectrum, the night minus day rate is $14.0\% \pm 6.3\%^{+1.5}_{-1.4}\%$ of the average rate. If the total flux of active neutrinos is additionally constrained to have no asymmetry, the $\nu_e$ asymmetry is found to be $7.0\% \pm 4.9\%^{+1.3}_{-1.2}\%$. A global solar neutrino

 0031-9007/02/89(1)/011302(5)$20.00  

analysis in terms of matter-enhanced oscillations of two active flavors strongly favors the large mixing angle solution.

DOI: 10.1103/PhysRevLett.89.011302 PACS numbers: 26.65.+t, 14.60.Pq, 95.85.Ry

The Sudbury Neutrino Observatory (SNO) has provided strong evidence that neutrinos change flavor as they propagate from the core of the Sun [1,2], independently of solar model flux predictions. This flavor conversion can be explained by neutrino oscillation models based on flavor mixing. For some values of the mixing parameters, spectral distortions and a measurable dependence on solar zenith angle are expected [3–5]. The latter might be caused by interaction with the matter of the Earth (the MSW effect) and would depend not only on oscillation parameters and neutrino energy, but also on the path length and $e^-$ density through the Earth. This Letter presents SNO's first measurements of day and night neutrino energy spectra, and constraints on allowed neutrino mixing parameters.

The data reported here were recorded between 2 November 1999 and 28 May 2001 UTC. The total live times for day and night are 128.5 and 177.9 days, respectively. The time-averaged inverse-square distance to the Sun $\langle(\frac{1\ \mathrm{AU}}{R})^2\rangle$ was 1.0002 (day) and 1.0117 (night). During the development of this analysis, the data were partitioned into two sets of approximately equal live time (split at 1 July 2000), each having substantial day and night components. Analysis procedures were refined during the analysis of Set 1 and fixed before Set 2 was analyzed. The latter thus served as an unbiased test. Unless otherwise stated, the analysis presented in this paper is for the combined data set.

The data reduction in [1] was used here. For each event, the number, pattern, and timing of the hit photomultiplier tubes (PMTs) were used to reconstruct effective recoil electron kinetic energy $T_{\mathrm{eff}}$, radial position $R$, and scattering angle $\theta_\odot$ with respect to the Sun-Earth direction. The charged current (CC), elastic scattering (ES), and neutral current (NC) reactions each have characteristic probability density functions (pdfs) of $T_{\mathrm{eff}}, R$, and $\theta_\odot$. A maximum likelihood fit of the pdfs to the data determined the flux from each of these reactions.

The measured night and day fluxes $\phi_N$ and $\phi_D$ were used to form the asymmetry ratio for each reaction: $\mathcal{A} = 2(\phi_N - \phi_D)/(\phi_N + \phi_D)$. The CC interaction is sensitive only to $\nu_e$. The NC interaction is equally sensitive to all active neutrino flavors, so active-only neutrino models predict $\mathcal{A}_{\mathrm{NC}} = 0$ [6]. The same models allow $\mathcal{A}_{\mathrm{CC}} \neq 0$. The ES reaction has additional contributions from $\nu_{\mu\tau}$ leading to a reduction in its sensitivity to $\nu_e$ asymmetries.

SNO used calibration sources [7] to constrain variations in detector response [8] that can lead to day-night asymmetries. A $^{16}$N source [9], which produces 6.1-MeV gamma rays, revealed a 1.3% per year drift in the energy scale. Because of seasonal variation in day and night live time, this drift can create an artificial asymmetry. The analysis corrected for this drift and a systematic uncertainty was assigned using worst-case drift models. Gamma rays from the $^{16}$N source were also used to constrain directional dependences in SNO's response.

A set of signals that are continuously present in the detector was used to probe possible diurnal variations in detector response. The detector was triggered at 5 Hz with a pulser, verifying live-time accounting. Muons provide an almost constant signal and, through interactions with $D_2O$, produce secondary neutrons. After applying a cut to remove bursts with high neutron multiplicity, these muon-induced neutrons were used to limit temporal variations in detector response. A more sensitive study focused on a solitary point of high background radioactivity, or "hot spot," on the upper hemisphere of the SNO acrylic vessel, apparently introduced during construction. Its event rate was stable and sufficient to make an excellent test of diurnal variations. It also provides a sensitive test for changes in reconstruction. A limit of 3.5% on the hot spot rate asymmetry was determined, which because of its steeply falling energy spectrum constrained the day and night energy scales to be the same within 0.3%. An east/west division of the neutrino data based on the Sun's position should show no rate variations from matter effects. As expected, the CC rates for east and west data were consistent. The rate asymmetries for each test are shown in Fig. 1.

Backgrounds were subtracted separately for day and night as part of the signal extraction. The results were normalized for an Earth-Sun distance of 1 AU, yielding the results in Table I. Day and night fluxes are given separately for data Sets 1 and 2, and for the combined data. A $\chi^2$ consistency test of the six measured fluxes between Sets 1 and 2 yielded a chance probability of 8%. A similar test done directly on the three asymmetry parameters gave a chance probability of 2%. No systematic has been identified, in either signal or background regions, that would

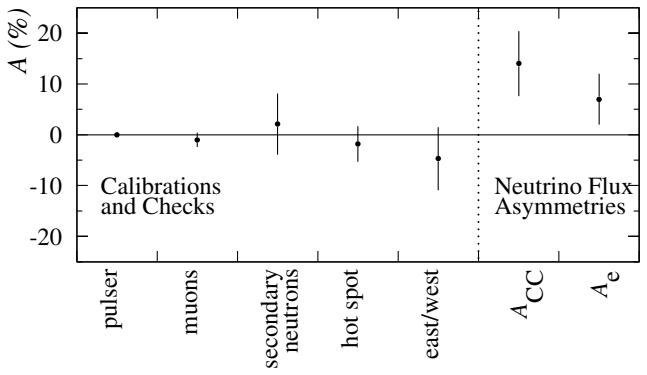


FIG. 1. Various event classes used to determine systematic differences between day and night measurements. Also shown are measured asymmetries on the CC flux, and on the electron neutrino flux derived from the CC, ES, and NC rates when the total neutrino flux is constrained to have zero asymmetry.

TABLE I. The results of signal extraction, assuming an undistorted $^8$B spectrum. The systematic uncertainties (combined set) include a component that cancels in the formation of the $\mathcal{A}$. Except for the dimensionless $\mathcal{A}$, the units are $10^6$ cm$^{-2}$ s$^{-1}$. Flux values have been rounded, but the asymmetries were calculated with full precision.

| | Set 1 | | Set 2 | | Combined | | |
|---|---|---|---|---|---|---|---|
| Signal | $\phi_D$ | $\phi_N$ | $\phi_D$ | $\phi_N$ | $\phi_D$ | $\phi_N$ | $\mathcal{A}(\%)$ |
| CC | 1.53 ± 0.12 | 1.95 ± 0.10 | 1.69 ± 0.12 | 1.77 ± 0.11 | 1.62 ± 0.08 ± 0.08 | 1.87 ± 0.07 ± 0.10 | $+14.0 \pm 6.3^{+1.5}_{-1.4}$ |
| ES | 2.91 ± 0.52 | 1.59 ± 0.38 | 2.35 ± 0.51 | 2.88 ± 0.47 | 2.64 ± 0.37 ± 0.12 | 2.22 ± 0.30 ± 0.12 | $-17.4 \pm 19.5^{+2.4}_{-2.2}$ |
| NC | 7.09 ± 0.97 | 3.95 ± 0.75 | 4.56 ± 0.89 | 5.33 ± 0.84 | 5.69 ± 0.66 ± 0.44 | 4.63 ± 0.57 ± 0.44 | $-20.4 \pm 16.9^{+2.4}_{-2.5}$ |

suggest that the differences between Set 1 and Set 2 are other than a statistical fluctuation. For the combined analysis, $\mathcal{A}_{\rm CC}$ is $+2.2\sigma$ from zero, while $\mathcal{A}_{\rm ES}$ and $\mathcal{A}_{\rm NC}$ are $-0.9\sigma$ and $-1.2\sigma$ from zero, respectively. Note that $\mathcal{A}_{\rm CC}$ and $\mathcal{A}_{\rm NC}$ are strongly statistically anticorrelated ($\rho = -0.518$), while $\mathcal{A}_{\rm CC}$ and $\mathcal{A}_{\rm ES}$ ($\rho = -0.161$) and $\mathcal{A}_{\rm ES}$ and $\mathcal{A}_{\rm NC}$ ($\rho = -0.106$) are moderatedly anticorrelated. Table II gives the systematic uncertainties on the asymmetry parameters. The day and night energy spectra for all accepted events are shown in Fig. 2.

Table III (a) shows the results for $\mathcal{A}_e$ derived from the CC day and night rate measurements, i.e., $\mathcal{A}_e = \mathcal{A}_{\rm CC}$. The day and night flavor contents were then extracted by changing variables to $\phi_{\rm CC} = \phi_e$, $\phi_{\rm NC} = \phi_{\rm tot} = \phi_e + \phi_{\mu\tau}$, and $\phi_{\rm ES} = \phi_e + \epsilon\phi_{\mu\tau}$, where $\epsilon \equiv 1/6.48$ is the ratio of the average ES cross sections above 5 MeV for $\nu_{\mu\tau}$ and $\nu_e$. Table III (b) shows the asymmetries of $\phi_e$ and $\phi_{\rm tot}$ with this additional constraint from the ES rate measurements. This analysis allowed for an asymmetry in the total flux of $^8$B neutrinos (nonzero $\mathcal{A}_{\rm tot}$), with the measurements of $\mathcal{A}_e$ and $\mathcal{A}_{\rm tot}$ having a strong anticorrelation. Figure 3 shows the $\mathcal{A}_e$ vs $\mathcal{A}_{\rm tot}$ joint probability contours. Forcing $\mathcal{A}_{\rm tot} = 0$, as predicted by active-only models, yielded the result in Table III (c) of $\mathcal{A}_e = 7.0\% \pm 4.9\%\ (\text{stat})^{+1.3}_{-1.2}\%\ (\text{syst})$.

The Super-Kamiokande (SK) collaboration measured $\mathcal{A}_{\rm ES}(\text{SK}) = 3.3\% \pm 2.2\%\ (\text{stat})^{+1.3}_{-1.2}\%\ (\text{syst})$ [10]. The ES measurement includes a neutral current component, which reduces the asymmetry for this reaction relative to $\mathcal{A}_e$ [11]. $\mathcal{A}_{\rm ES}$(SK) may be converted to an equivalent electron flavor asymmetry using the total neutrino flux measured by SNO, yielding $\mathcal{A}_e$(SK) [Table III (d)]. This value is in good agreement with SNO's direct measurement of $\mathcal{A}_e$, as seen in Fig. 3.

SNO's day and night energy spectra (Fig. 2) have also been used to produce MSW exclusion plots and limits on neutrino flavor mixing parameters. MSW oscillation models [12] between two active flavors were fit to the data. For simplicity, only the energy spectra were used in the fit, and the radial $R$ and direction $\cos\theta_\odot$ information was omitted. This procedure preserves most of the ability to discriminate between oscillation solutions. A model was constructed for the expected number of counts in each energy bin by combining the neutrino spectrum [13], the survival probability, and the cross sections [14] with SNO's response functions [8]. For this analysis, the dominant systematics are those for the combined fluxes, as detailed in Refs. [1,8], and not the diurnal systematics of Table II.

There are three free parameters in the fit: the total $^8$B flux $\phi_B$, the difference $\Delta m^2$ between the squared

TABLE II. Effect of systematic uncertainties on $\mathcal{A}$ (%). For presentation, uncertainties have been symmetrized and rounded.

| Systematic | $\delta\mathcal{A}_{\rm CC}$ | $\delta\mathcal{A}_{\rm ES}$ | $\delta\mathcal{A}_{\rm NC}$ |
|---|---|---|---|
| Long-term energy scale drift | 0.4 | 0.5 | 0.2 |
| Diurnal energy scale variation | 1.2 | 0.7 | 1.6 |
| Directional energy scale variation | 0.2 | 1.4 | 0.3 |
| Diurnal energy resolution variation | 0.1 | 0.1 | 0.3 |
| Directional energy resolution variation | 0.0 | 0.1 | 0.0 |
| Diurnal vertex shift variation | 0.5 | 0.6 | 0.7 |
| Directional vertex shift variation | 0.0 | 1.1 | 0.1 |
| Diurnal vertex resolution variation | 0.2 | 0.7 | 0.5 |
| Directional angular reconstruction variation | 0.0 | 0.1 | 0.1 |
| PMT $\beta$-$\gamma$ background | 0.0 | 0.2 | 0.5 |
| AV + $H_2O$ $\beta$-$\gamma$ background | 0.0 | 0.6 | 0.2 |
| $D_2O$ $\beta$-$\gamma$, neutrons background | 0.1 | 0.4 | 1.2 |
| External neutrons background | 0.0 | 0.2 | 0.4 |
| Cut acceptance | 0.0 | 0.2 | 0.4 |
| Total | 1.5 | 2.4 | 2.4 |

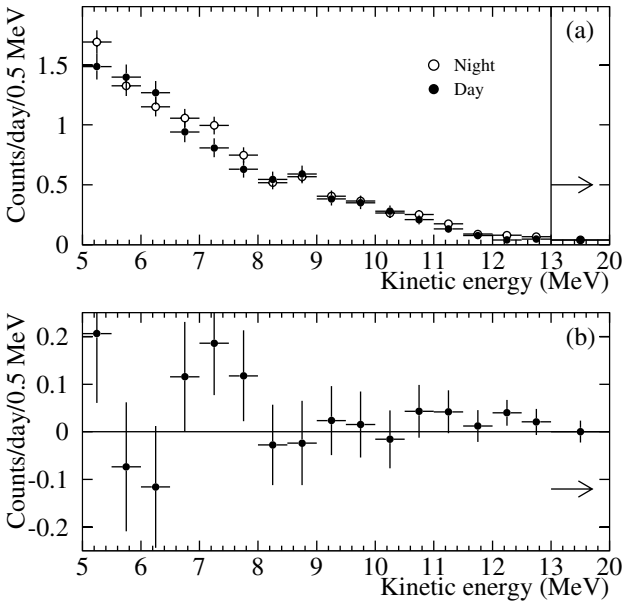


FIG. 2. (a) Energy spectra for day and night. All signals and backgrounds contribute. The final bin extends from 13.0 to 20.0 MeV. (b) Difference, night − day, between the spectra. The day rate was 9.23 ± 0.27 events/day, and the night rate was 9.79 ± 0.24 events/day.

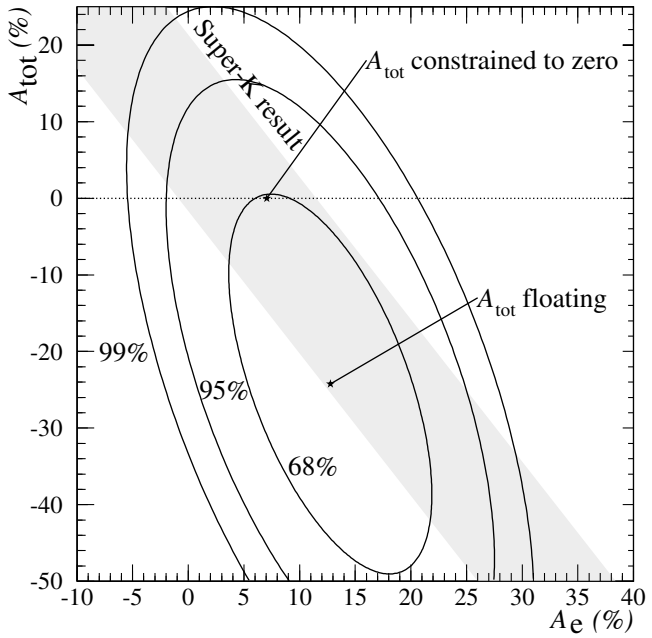


FIG. 3. Joint probability contours for $\mathcal{A}_{\rm tot}$ and $\mathcal{A}_e$. The points indicate the results when $\mathcal{A}_{\rm tot}$ is allowed to float and when it is constrained to zero. The diagonal band indicates the 68% joint contour for the Super-K $\mathcal{A}_{\rm ES}$ measurement.

masses of the two neutrino mass eigenstates, and the mixing angle $\theta$. The flux of higher energy neutrinos from the solar *hep* reaction was fixed at $9.3 \times 10^3$ cm$^{-2}$ s$^{-1}$ [15]. Contours were generated in $\Delta m^2$ and $\tan^2\theta$ for $\Delta\chi^2$(C.L.) = 4.61(90%), 5.99(95%), 9.21(99%), and 11.83 (99.73%). Figure 4(a) shows allowed mixing parameter regions using only SNO data with no additional experimental constraints or inputs from solar models. By including flux information from the Cl [16] and Ga experiments [17–21], the day and night spectra from the SK experiment [10], along with solar model predictions for the more robust *pp*, *pep*, and $^7$Be neutrino fluxes [15], the contours shown in Fig. 4(b) were produced. This global analysis strongly favors the large mixing angle (LMA) region (see Table IV), and $\tan^2\theta$ values $<1$. While the absolute chi-squared per degree of freedom is not particularly large for the LOW solution, the difference between chi-squared values still reflects the extent to which one region of MSW parameter space is favored compared to another. Repeating the global analysis using the total SNO energy spectrum instead of separate day and night spectra gives nearly identical results.

In summary, SNO has measured the day-night asymmetries of the CC, NC, and ES reaction rates. From these

TABLE III. Measurement of the $\phi_e$ and $\phi_{\rm tot}$ asymmetry for various constraints. All analyses assume an undistorted $^8$B spectrum.

| Constraints | Asymmetry (%) |
|---|---|
| (a) No additional constraint | $\mathcal{A}_{\rm CC} = 14.0 \pm 6.3^{+1.5}_{-1.4}$<br>$\mathcal{A}_{\rm NC} = -20.4 \pm 16.9^{+2.4}_{-2.5}$<br>(see text for correlations) |
| (b) $\phi_{\rm ES} = (1-\epsilon)\phi_e + \epsilon\phi_{\rm tot}$ | $\mathcal{A}_e = 12.8 \pm 6.2^{+1.5}_{-1.4}$<br>$\mathcal{A}_{\rm tot} = -24.2 \pm 16.1^{+2.4}_{-2.5}$<br>Correlation $= -0.602$ |
| (c) $\phi_{\rm ES} = (1-\epsilon)\phi_e + \epsilon\phi_{\rm tot}$<br>$\mathcal{A}_{\rm tot} = 0$ | $\mathcal{A}_e = 7.0 \pm 4.9^{+1.3}_{-1.2}$ |
| (d) $\phi_{\rm ES} = (1-\epsilon)\phi_e + \epsilon\phi_{\rm tot}$<br>$\mathcal{A}_{\rm tot} = 0$<br>$\mathcal{A}_{\rm ES}$(SK) $= 3.3\% \pm 2.2\%^{+1.3}_{-1.2}\%$ | $\mathcal{A}_e$(SK) $= 5.3 \pm 3.7^{+2.0}_{-1.7}$<br>(derived from SK $\mathcal{A}_{\rm ES}$<br>and SNO total $^8$B flux) |

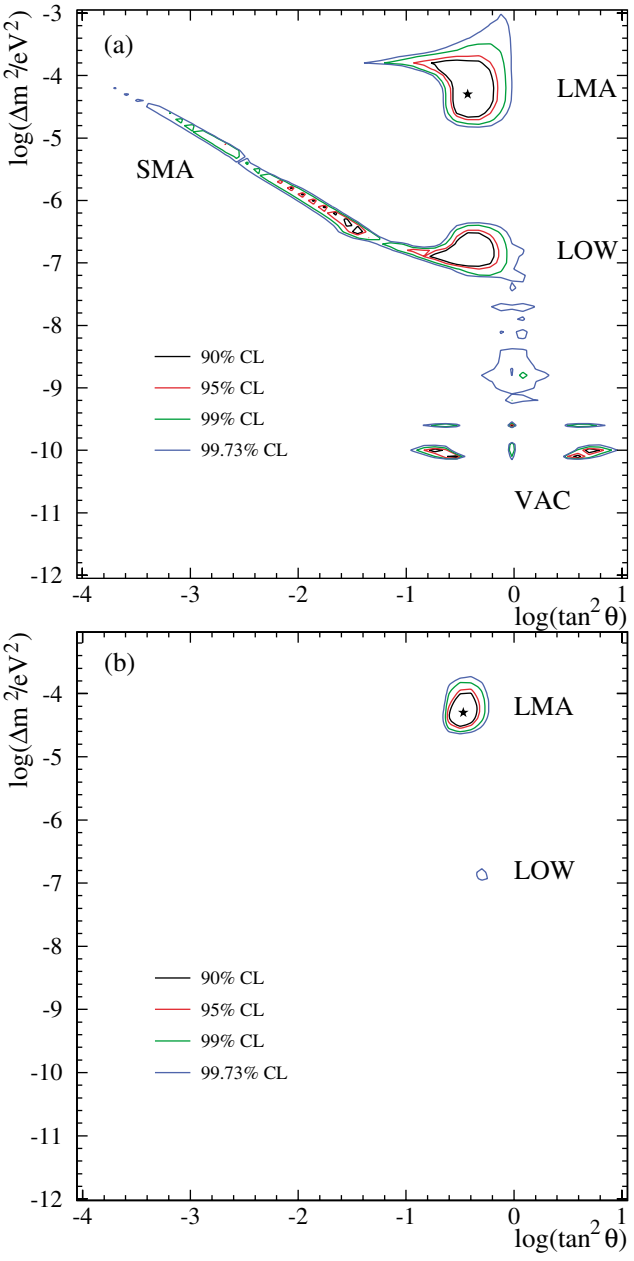


FIG. 4 (color). Allowed regions of the MSW plane determined by a $\chi^2$ fit to (a) SNO day and night energy spectra and (b) with additional experimental and solar model data. The star indicates the best fit. See text for details.

TABLE IV. Best-fit points in the MSW plane for global MSW analysis using all solar neutrino data. $\phi_B$ is the best-fit $^8$B flux for each point, and has units of $10^6$ cm$^{-2}$ s$^{-1}$. $\Delta m^2$ has units of eV$^2$. $\mathcal{A}_e$ is the predicted asymmetry for each point.

| Region | $\chi^2_{\min}$/dof | $\phi_B$ | $\mathcal{A}_e$(%) | $\Delta m^2$ | $\tan^2\theta$ | C.L.(%) |
|---|---|---|---|---|---|---|
| LMA | 57.0/72 | 5.86 | 6.4 | $5.0 \times 10^{-5}$ | 0.34 | ··· |
| LOW | 67.7/72 | 4.95 | 5.9 | $1.3 \times 10^{-7}$ | 0.55 | 99.5 |

results, the first direct measurements of the day-night asymmetries in the $\nu_e$ flux and the total $\nu$ flux from the Sun have been deduced. A global fit to SNO's day and night energy spectra and data from other solar neutrino experiments strongly favors the LMA solution in a two-flavor MSW neutrino oscillation analysis.

This research was supported by Canada: NSERC, Industry Canada, NRC, Northern Ontario Heritage Fund Corporation, INCO, AECL, Ontario Power Generation; U.S.: Department of Energy; U.K.: PPARC. We thank the SNO technical staff for their strong contributions.

*Permanent address: Birkbeck College, University of London, Malet Road, London WC1E 7HX, UK.
†Deceased.

[1] Q. R. Ahmad *et al.,* preceding Letter, Phys. Rev. Lett. **89**, 011301 (2002).
[2] Q. R. Ahmad *et al.,* Phys. Rev. Lett. **87**, 071301 (2001).
[3] S. P. Mikheyev and A. Y. Smirnov, in *Proceedings of the Moriond Workshop, 1986,* edited by O. Fackler and J. Tran Thanh Van (Editions Frontières, Gif-sur-Yvette, France, 1986), p. 335.
[4] A. J. Baltz and J. Weneser, Phys. Rev. D **37**, 3364 (1988).
[5] M. C. Gonzalez-Garcia, C. Peña-Garay, and A. Y. Smirnov, Phys. Rev. D **63**, 113004 (2001).
[6] A nonzero value for $\mathcal{A}_{\rm NC}$ might be evidence for sterile neutrinos.
[7] SNO Collaboration, J. Boger *et al.,* Nucl. Instrum. Methods Phys. Res., Sect. A **449**, 172 (2000).
[8] Details of SNO response functions are available from the SNO web site: http://sno.phy.queensu.ca
[9] M. Dragowsky *et al.,* Nucl. Instrum. Methods Phys. Res., Sect. A **481**, 284 (2002).
[10] S. Fukuda *et al.,* Phys. Rev. Lett. **86**, 5651 (2001).
[11] J. N. Bahcall, P. Krastev, and A. Y. Smirnov, Phys. Rev. D **62**, 093004 (2000); M. Maris and S. T. Petcov, Phys. Rev. D **62**, 093006 (2000); J. N. Bahcall, M. C. Gonzalez-Garcia, and C. Peña-Garay, hep-ph/0111150 v2, 2002.
[12] S. J. Parke, Phys. Rev. Lett. **57**, 1275 (1986); S. T. Petcov, Phys. Lett. B **200**, 373 (1988); G. L. Fogli and E. Lisi, Astropart. Phys. **3**, 185 (1995); E. Lisi, A. Marrone, D. Montanino, A. Palazzo, and S. T. Petcov, Phys. Rev. D **63**, 093002 (2001).
[13] C. E. Ortiz *et al.,* Phys. Rev. Lett. **85**, 2909 (2000).
[14] S. Nakamura *et al.,* nucl-th/0201062.
[15] J. N. Bahcall, H. M. Pinsonneault, and S. Basu, Astrophys. J. **555**, 990 (2001).
[16] B. T. Cleveland *et al.,* Astrophys. J. **496**, 505 (1998).
[17] J. N. Abdurashitov *et al.,* Phys. Rev. C **60**, 055801 (1999).
[18] J. N. Abdurashitov *et al.,* astro-ph/0204245.
[19] M. Altmann *et al.,* Phys. Lett. B **490**, 16 (2000).
[20] W. Hampel *et al.,* Phys. Lett. B **447**, 127 (1999).
[21] C. M. Cattadori *et al.,* in Proceedings of the TAUP 2001 Workshop, 2001, Assergi, Italy.